

Extreme Ultraviolet Observations from Voyager 1 Encounter with Jupiter

Abstract. Observations of the optical extreme ultraviolet spectrum of the Jupiter planetary system during the Voyager 1 encounter have revealed previously undetected physical processes of significant proportions. Bright emission lines of S III, S IV, and O III indicating an electron temperature of 10^5 K have been identified in preliminary analyses of the Io plasma torus spectrum. Strong auroral atomic and molecular hydrogen emissions have been observed in the polar regions of Jupiter near magnetic field lines that map the torus into the atmosphere of Jupiter. The observed resonance scattering of solar hydrogen Lyman α by the atmosphere of Jupiter and the solar occultation experiment suggest a hot thermosphere (≥ 1000 K) with a large atomic hydrogen abundance. A stellar occultation by Ganymede indicates that its atmosphere is at most an exosphere.

The two Voyager spacecraft carry ultraviolet (UV) spectrometers designed to observe planetary atmospheres in the region 500 to 1700 Å (*1*). Observations of the Jupiter system with Voyager 1 began in early January 1979. The early spectra contain a spectacular mix of radiation from ionized and neutral atoms and molecules. Many of the physical processes implied by the observations are startling and carry implications that go far beyond expectations based on previous studies. The results reported here emphasize the many complex physical processes controlling the extended atmosphere and magnetosphere. The observed emissions are due to solar resonance scattering and particle impact in the Jupiter atmosphere and to high-temperature plasma processes in a plasma torus at the orbit of Io and in the magnetosphere extending out to the bow shock region. Although not all of the significant results are presented here, it is clear that the Voyager extreme ultraviolet (EUV) instruments have made significant discoveries related to both the up-

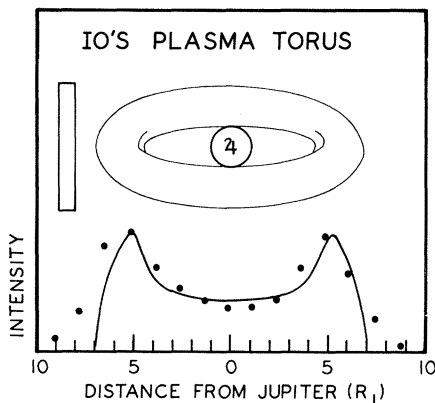


Fig. 1. The data points show the measured intensity of the 685-Å feature as a function of distance from Jupiter measured in the orbital plane of the satellites. A model torus used to fit the data is shown to scale above the data; the intensity predicted by this model is shown by the solid line. Other observations show intensities at eastern and western elongation points differing by a factor of up to 2.

per atmosphere and the magnetosphere of the planetary system. The pre-encounter observations have, in fact, provided the first observations of optical effects in the vicinity of the bow shock and magnetopause, opening a new area of study of the bow shock and magnetospheric processes. Spectra of the extended planetary system will be presented in forthcoming publications.

Bright emission lines in the vicinity of 685 and 833 Å appeared prominently in the spectrum of the Jupiter system on the first day of observation at a range of about 1 AU. Subsequent observations have defined the spatial distribution of the emitters as approximating a torus at the orbital distance of Io. The presence of bright emission features at this energy marks the discovery of a high-temperature plasma. Less energetic phenomena involving Na I and S II have been known for some time (*2*). The emitters identified to date are S III, S IV, and O III.

The spatial extent of the plasma torus has been defined by scanning the Jupiter system with the spectrometer slit oriented both parallel to and approximately perpendicular to the plane of the satellite orbits. The intensity of the 685-Å feature as a function of position in the satellite plane is shown in Fig. 1. The size and shape of the torus have been estimated by adjusting a crude model of it to obtain an acceptable fit to the data. This model consists of a toroidal cloud of uniform density with a radius of symmetry of 5.9 ± 0.3 Jupiter radii (R_J) and a cross-sectional radius of $1 \pm 0.3 R_J$. The plasma torus is centered on the magnetic equatorial plane and, therefore, moves up and down relative to the orbit of Io by the dipole offset angle of 10° . The excursion of Io above and below the magnetic equatorial plane, $1 R_J$, is the same as the observed vertical extent of the torus. It is reasonable to consider Io as a source, filling a volume of the magnetosphere with the emitting species. The ions are confined near the magnetic equatorial

plane because the pitch angle of a newly ionized atom is near 90° .

A typical spectrum from the plasma torus is shown in Fig. 2. The brightness of the features vary with time by as much as a factor of 2 with no apparent relationship to the position of Io. Although the major emission features of the torus are always present, the spectral content of data obtained at different times and at different positions also varies.

Model calculations, assuming an optically thin plasma in collisional ionization equilibrium, account for the major emission features of Fig. 2, with an appropriate mixture of S III, S IV, and O III. The spectra contain additional weaker emissions not yet identified. The relative brightness of the S III and S IV lines in the spectrum indicates a thermal electron temperature of 10^5 K. The strong multiplets of S III, 700 Å ($3p^2 \ ^3P-3d \ ^3P^0$), 683 Å ($3p^2 \ ^3P-4s \ ^3P^0$), and 680 Å ($3p^2 \ ^3P-3d \ ^3D^0$), dominate the feature at about 685 Å in the observed spectrum, with a contribution from the O III multiplet at 703 Å ($2p^2 \ ^3P-2p^3 \ ^3P^0$). The S III 1020 Å ($3p^2 \ ^3P-3p^3 \ ^3P^0$) transitions account for the feature at 1020 Å. The S IV multiplet ($3p \ ^3P-3p^2 \ ^3D$) is the feature at 1070 Å, and other S IV multiplets make a small contribution to the blend of lines around 685 Å. The prominent feature at 833 Å contains a blend of S III and S IV lines at 825 and 836 Å and O III at 834 Å. The relative brightness of the lines contributing to the 833-Å feature appears to be variable, but analysis of this particular spectrum suggests that the O III transition is dominant. The spectrum shows no indication of the prominent 539-Å transi-

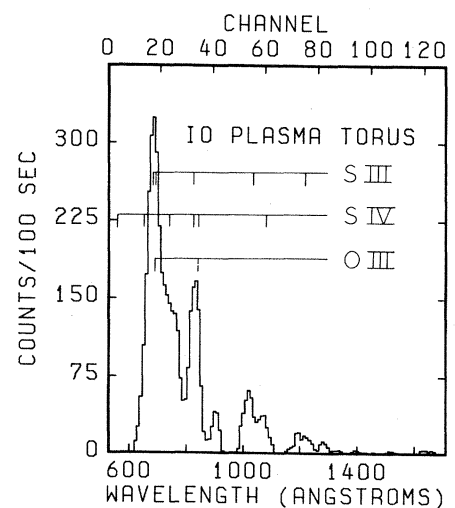


Fig. 2. Spectrum of the radiation from the plasma torus at elongation; sky background and instrumental scattering have been removed. Some lines of identified species are indicated in the spectrum. The feature at 685 Å is dominated by S III and has a brightness of 200 R.

tion of O II or the 554- and 608-Å transitions of O IV, suggesting low relative populations of these species. The weakness of the O II and O IV transitions is another indication of a plasma electron temperature near 10^5 K. Charge neutrality in the model requires a minimum electron density of $N_e \geq 2100 \text{ cm}^{-3}$. On that basis we estimate $[\text{S III}] \leq 95 \text{ cm}^{-3}$, $[\text{S IV}] \leq 55 \text{ cm}^{-3}$, and $[\text{O III}] \leq 850 \text{ cm}^{-3}$. If the preliminary electron density estimates obtained from plasma frequency measurements by Warwick *et al.* (3) are correct, the implication of the EUV observations is that oxygen and sulfur are the dominant species in the plasma torus. However, because of the observed temporal variations in the radiation from the torus, the electron density measured in situ may not represent the average conditions of the plasma inferred from the UV spectrometer observations. A different electron density could permit the presence of additional ionized species to be consistent with the UV data.

On the basis of these calculations, the radiative cooling rate of the torus due to S III emission alone amounts to $\sim 7 \times 10^{11}$ W. We conservatively estimate the total radiative cooling rate due to all species at $\sim 2 \times 10^{12}$ W. Energy must be continually supplied to the torus at least at this rate. A possible energy source mechanism is discussed below.

In view of the spatial distribution of the torus and the suggestive surface properties and volcanic activity of Io, it seems reasonable to assume that the satellite is the dominant source of particles for the plasma. Neutral particles entering the torus under the model conditions described above are ionized with a probability of $\sim 1.5 \times 10^{-6} \text{ sec}^{-1}$ by the plasma electrons. The ions are accelerated by Jupiter's magnetic field to a relative speed of 56 km/sec. The ion acquires a guiding center drift equal to the magnetic field corotation rate and a gyrospeed around the guiding center equal to the corotation speed in the Io frame of reference (4). Sulfur and oxygen ions acquire 520 and 260 eV, respectively, from the magnetic field. This energy is available for heating the electrons and for further ionization to the equilibrium condition. If we assume this mechanism is the dominant energy source, the radiative loss rate given above requires the introduction and loss of $\sim 1.4 \times 10^{-4}$ sulfur ions per cubic centimeter per second. This implies a lifetime of 10^6 seconds and requires that Io supply a sulfur and oxygen ion flux of $\sim 10^{10} \text{ cm}^{-2} \text{ sec}^{-1}$ (5).

Callisto. The airglow observations at closest approach to the satellites were

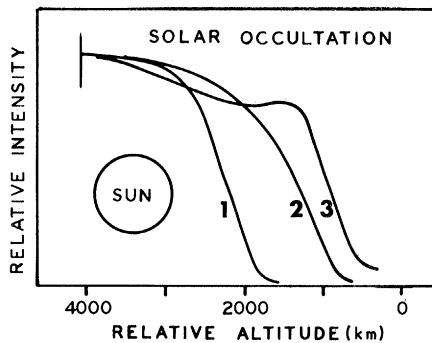


Fig. 3. Relative intensity versus altitude, showing atmospheric absorption during the solar occultation experiment. The reference altitude is arbitrary and the scales are linear. Altitude displacement of the light curves indicates a hot hydrogen upper atmosphere. (Curve 1) 600 to 800 Å; (curve 2) 900 to 1150 Å; (curve 3) 1425 to 1675 Å.

designed to measure the scale height of a gravitationally bound atmosphere. The emission observed is assumed to arise from resonance scattering of sunlight or particle impact excitation. The instrument is sensitive to emission from most atomic species, including oxygen, helium, and hydrogen. Preliminary analysis indicates no measurable emission in the range 500 to 1700 Å. An upper limit to the surface density of O I at $5 \times 10^6 \text{ cm}^{-3}$ has been estimated from a calculation of solar resonance scattering. An upper limit for the He density of $8 \times 10^4 \text{ cm}^{-3}$ has been estimated on the same basis. The measurement of atomic hydrogen emission is complicated by uncertainties in the contribution of the background signal and a meaningful estimate awaits further analysis.

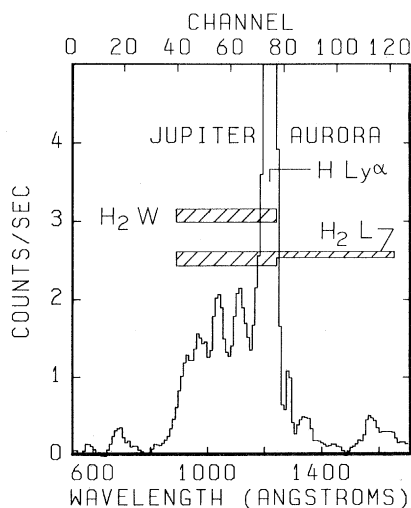


Fig. 4. Spectrum of emission from the circumpolar auroral regions on Jupiter. The Ly α line is artificially enhanced over the auroral spectrum by resonance scattering of solar Ly α because at this time the auroral zone is smaller than the field of view. The emission in the wavelength range 900 to 1130 Å is from H₂ Lyman and Werner bands, as indicated.

Ganymede. The UV spectrometer observed the moderately bright UV star Kappa Centauri as it was occulted by Ganymede. A stellar radiation source is limited to wavelengths longer than the hydrogen absorption edge at 912 Å, and therefore the observation with our instrument is only applicable to atmospheric constituents that have an appreciable absorption cross section between 912 and 1700 Å, such as O₂, H₂O, CO₂, and CH₄. No signature in the recorded stellar spectrum was attributable to extinction of the stellar radiation by an atmospheric constituent of the satellite. We believe that a 10 percent extinction of the source intensity would have been detectable. This allows us to place an upper limit of $6 \times 10^8 \text{ cm}^{-3}$ on the surface density of any appropriate atmospheric constituent. This upper limit of 10^{-8} mbar is much lower than the measurement reported by Carlson *et al.* (6) of an atmosphere with a surface pressure of at least 10^{-3} mbar.

Jupiter's atmosphere. Use of the sun as the radiation source to probe a planetary or satellite atmosphere has an advantage over the use of a stellar source, as described above for Ganymede. The sun has emission throughout the spectral range, 500 to 1700 Å, of our instrument. The spectral range from 500 to 900 Å is particularly useful since all common atmospheric gases or their photochemical products have large absorption cross sections within it (7, 8). In the case of Jupiter, the dominant absorbers throughout the spectral region are already known and are given in detail in the experiment description by Broadfoot *et al.* (1). The experiment was successful, as explained below, but further analysis will require extensive modeling.

The light curves in Fig. 3 represent three regions of the spectrum in which we expect absorption by three or four different atmospheric constituents. Curve 1 is a summation of intensity over the spectral range 600 to 800 Å dominated by H₂ absorption. Curve 2 shows the CH₄ absorption region, 900 to 1150 Å. Finally, curve 3 represents the region 1425 to 1675 Å, where we expect a combination of C₂H₂ and C₂H₆ to be most effective. The apparent size of the sun as an atmospheric probe at the limb of the planet is also shown. The angular size of the sun is large and controls the slope of the attenuation to a great extent. The altitude shift between the light curves is the signature of most interest. The structure that is evident in the upper parts of the curves involves the details of extinction. The lower sections of the curves, where the slopes are similar,

show the strong effect of the absorption characteristics of the gas. In the experiment description (1) we showed altitude differences of about 200 km in these representative spectral regions. In Fig. 3, one has the impression that there are differences of 1000 km between the H₂ and CH₄ regions and 350 km between the lower two regions. This observation alone implies a much more extensive altitude distribution than our reference model (1). We suggest a thermospheric temperature greater than 1000 K. This is consistent with our preliminary analysis of the resonance-scattered disk intensity, discussed below.

The scale height and identification of the absorbers can be obtained from this experiment. Just as there are shifts in the light curves over the broad spectral regions shown in Fig. 3, similar but smaller shifts will be evident in narrower wavelength bands within the wavelength region dominated by a single absorber. The higher degree of differentiation provided by greater wavelength resolution in the data is expected to result in estimates of the constituent scale heights.

The prominent UV radiation from the atmosphere of Jupiter can be divided into two categories: (i) disk emission, which is predominantly resonance-scattered solar hydrogen Lyman α (Ly α) emission, and (ii) auroral emission, which is concentrated in the polar regions, excited by high-energy particle precipitation along the magnetic field lines. Figure 4 shows a spectrum with the characteristic features of both categories. The strong disk and auroral feature at 1216 Å, which runs off scale, is the hydrogen Ly α line. The H₂ band emission between 900 and 1130 Å is characteristic of the auroral region. Figure 5 shows the relative intensity of both of these features across the disk. The geometry of the observation is illustrated on the right side of Fig. 5; the slit is tangent to the pole and moves slowly from pole to pole. The Ly α intensity profile shows an auroral enhancement at the poles and a disk brightness that increases toward the center. The H₂ emission in the region 900 to 1130 Å is also shown; strong emission was present only in the aurora near the poles.

A better data set representative of the Ly α intensity variation over the disk is shown in Fig. 6. Since the dark side of the planet radiates less than 700 rayleighs (R), which limits the intensity due to particle precipitation over the planet, we conclude that the measured disk emission of up to 20 kR is predominantly resonance-scattered sunlight. Preliminary calculations support

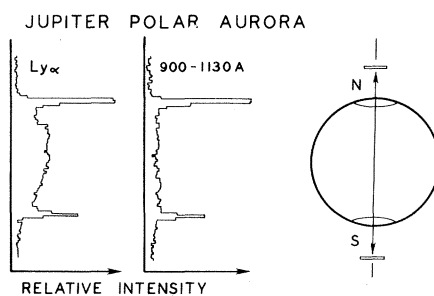


Fig. 5. Intensity variations in two wavelength bands that include auroral emissions define the position of Jupiter's auroral zones near the poles, but clearly distinct from the polar limbs. The width of the auroral zone in the meridian plane is significantly less than the 7000-km width of the projected spectrometer slit.

this conclusion. Detailed radiative transfer calculations (9) for a variety of thermospheric models indicate that the Ly α brightness measured here requires a thermospheric temperature ≈ 1000 K, an eddy diffusion coefficient $K < 10^6$ cm²/sec, and a hydrogen column density above the CH₄ turbopause $\approx 10^{18}$ cm⁻². These values are in contrast to $K \sim 3 \times 10^7$ cm²/sec and lower hydrogen densities implied by Pioneer 10 UV photometer data (10). The computed center-to-limb variation is proportional to the cosine of the solar zenith angle out to 60°, in agreement with the observed variation in Fig. 6. The solar Ly α flux at 1 AU at the time of encounter was assumed to be 3.75×10^{11} photons per square centimeter per second (11), the value used to analyze Pioneer Venus UV data (12). An upper limit on the intensity of He (584 Å) radiation of 0.1 R is suggested by the disk spectra analyzed to

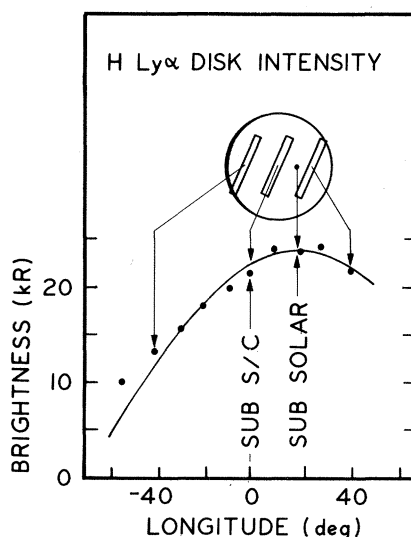


Fig. 6. Variation of the resonance-scattered hydrogen Ly α intensity with position on the planet. The curved line shows a cosine dependence about the subsolar point; S/C denotes spacecraft.

date. The absence of a detectable He emission is compatible with the thermospheric structure deduced from the Ly α brightness. The remarkable difference between the Voyager and Pioneer 10 UV measurements may reflect substantial variability in Jupiter's thermosphere in response to solar activity or interaction with the magnetosphere and Io's plasma torus, or both.

The auroral spectrum (Fig. 4) has features that will prove to be useful atmospheric diagnostic signatures, although the detailed analysis is beyond the scope of this report. The relative intensities of the He, H, and H₂ bands, due to impact excitation, are well known. In particular, the data suggest that emissions from He, H₂, and H are modified by absorption along the path to the spacecraft. We expect to determine the number density of both H and H₂ along the path to the auroral emission source deep in the atmosphere.

The location of the auroral emission at about 65° latitude is consistent with the mapping of Io's plasma torus into the atmosphere along the magnetic field. This fact, taken with the absence of comparable auroral excitation elsewhere, suggests that the plasma torus may play a key role in determining the morphology of the auroral regions. The north-south asymmetry in auroral intensity may be related to the differing field strengths at the northern and southern ends of the field lines threading the torus. Since these bright auroral regions around the poles include the expected locations of the foot of Io's flux tube (13), they would tend to obscure the presence of any strong localized atmosphere-magnetosphere interaction due to the flux tube. At the time of this observation, the predicted location of the foot of Io's flux tube was on the far side of the planet.

Discussion. A comparison of the picture of the Jovian system presented here with that based on the Pioneer 10 UV photometer observations shows two general areas of marked contrast; the disk brightness of Jupiter and the intensity of the emission from the plasma torus. Because of the remarkable differences in both of these areas, we conclude that the Jupiter-Io environment has changed significantly since December 1973. The observed differences are so spectacularly large that this conclusion does not require a detailed comparison of the two instruments, their calibrations, or the observing geometry. The primary UV observations of Jupiter from Pioneer 10 were taken about 46 R_J from the planet. The Voyager UV spectrometers had a similar viewing geometry at 460 R_J (33

days before encounter). The spatial resolution would allow either instrument to separate the orbital and planetary emissions. In interpreting the Pioneer 10 UV observations, Carlson and Judge (10) assumed that all of the signal in the long-wavelength channel when Jupiter was in the field was due to hydrogen Ly α . Based on this assumption, the disk-averaged brightness was 400 R. The Voyager UV spectrometer measurement of hydrogen Ly α radiation was 14 kR averaged over the disk, a factor of 35 greater than the Pioneer 10 value. With the elongation point of Io's orbit in the field of view of the Pioneer 10 UV photometer, a signal in the long-wavelength channel was interpreted as 300 R of Ly α . No measurable emission was recorded in the short-wavelength channel (200 to 800 Å). The Voyager UV spectrometers recorded as much as 200 R in a single feature at 685 Å in the torus. This emission would have resulted in a prominent signal in both the UV photometer channels of Pioneer 10. We are satisfied that the Jupiter-Io system has undergone a major change since the Pioneer 10 encounter.

The results suggest that a high-temperature plasma torus was not present during the Pioneer 10 encounter in 1973 and that auroral activity was probably at a low level. These observations are consistent with a relationship between the presence of the plasma torus and auroral activity in the atmosphere of Jupiter, as suggested above.

Other evidence for major temporal changes in the Jupiter spectrum is found in the various measurements of hydrogen Ly α emission. The differences among these measurements appear to go beyond experimental uncertainties. Measurements from the Copernicus satellite (14) and earlier rocket measurements (15) range from 1.2 to 4 kR. More recent rocket measurements (16) (1 December 1978) produced a disk-averaged brightness of 13 kR. A measurement with the International Ultraviolet Explorer Instrument (16) on 9 December 1978 provided a subsolar brightness (averaged over 11×23 arc-seconds) of 12 to 14 kR, in substantial agreement with the Voyager UV spectrometer observations. Apparent variations in UV planetary albedo have also been recorded in earlier work (17).

It is clear that continuing Earth-based observations are necessary to aid our understanding the variability of the planetary system. Periodic observations of the Jupiter disk and polar auroral regions in H and H₂ emission are recommended, along with UV albedo measurements at longer wavelengths. The Io plasma torus

is of special interest and attempts should be made to observe some of the emission characteristics of the higher-temperature components. The Voyager UV spectrometer data base on the torus will ultimately span a period of a least 2 years.

A. L. BROADFOOT

M. J. S. BELTON, P. Z. TAKACS
*Kitt Peak National Observatory,
Tucson, Arizona 85726*

B. R. SANDEL, D. E. SHEMANSKY
*Space Sciences Institute, University
of Southern California Tucson
Laboratories, Tucson, Arizona 85713*

J. B. HOLBERG
*Planetary Science Institute,
Pasadena, California 91101*

J. M. AJELLO
*Jet Propulsion Laboratory,
Pasadena, California 91103*

S. K. ATREYA, T. M. DONAHUE
University of Michigan, Ann Arbor 48109

H. W. MOOS
*Johns Hopkins University,
Baltimore, Maryland 21218*

J. L. BERTAUX, J. E. BLAMONT
*Service d'Aeronomie du CNRS,
Paris, France*

D. F. STROBEL
*Naval Research Laboratory,
Washington, D.C. 20375*

J. C. MCCONNELL
*York University,
Ontario, Canada M3J 1P3*

A. DALGARNO
R. GOODY, M. B. MCELROY
*Harvard University,
Cambridge, Massachusetts 02138*

References and Notes

1. A. L. Broadfoot *et al.*, *Space Sci. Rev.* **21**, 183 (1977).
2. R. A. Brown and Y. L. Yung, in *Jupiter*, T. Gehrels, Ed. (Univ. of Arizona Press, Tucson, 1976), p. 1102.
3. J. W. Warwick, J. B. Pearce, R. G. Peltzer, A. C. Riddle, *Science* **204**, 995 (1979).
4. G. L. Siscoe and C. K. Chen, *Icarus* **31**, 1 (1977).
5. B. A. Smith, L. A. Soderblom, T. V. Johnson, A. P. Ingersoll, S. A. Collins, E. M. Shoemaker, G. E. Hunt, H. Masursky, M. H. Carr, M. E. Davies, A. F. Cook II, J. Boyce, G. E. Danielson, T. Owen, C. Sagan, R. F. Beebe, J. Ververka, R. G. Strom, J. F. McCauley, D. Morrison, G. A. Briggs, V. E. Suomi, *Science* **204**, 951 (1979).
6. R. W. Carlson, J. C. Bhattacharya, B. A. Smith, T. V. Johnson, B. Hidayat, S. A. Smith, G. E. Taylor, B. O'Leary, R. T. Brinkmann, *ibid.* **182**, 53 (1973).
7. A. L. Broadfoot, S. S. Clapp, F. E. Stuart, *Space Sci. Instrum.* **3**, 209 (1977).
8. A. L. Broadfoot, S. Kumar, M. J. S. Belton, M. B. McElroy, *Science* **185**, 166 (1974).
9. Y. L. Yung and D. F. Strobel, in preparation.
10. R. W. Carlson and D. L. Judge, *J. Geophys. Res.* **79**, 3623 (1974).
11. A. Vidal-Madjar, *Solar Phys.* **40**, 69 (1975).
12. A. I. Stewart, D. E. Anderson, Jr., L. W. Esposito, C. A. Barth, *Science* **203**, 777 (1979).
13. M. H. Acuña and N. F. Ness, *J. Geophys. Res.* **81**, 2917 (1976).
14. S. K. Atreya, Y. L. Yung, T. M. Donahue, E. S. Barker, *Astrophys. J.* **218**, L83 (1977).
15. G. J. Rottman, H. W. Moos, C. S. Freer, *ibid.* **184**, L89 (1973).
16. J. T. Clarke, W. G. Fastie, P. D. Feldman, H. W. Moos, H. A. Weaver, C. B. Opal, *Eos*, in press.
17. R. C. Anderson, J. G. Pipes, A. L. Broadfoot, L. Wallace, *J. Atmos. Sci.* **26**, 874 (1969).
18. We acknowledge the untiring effort of Susan Hanson, our Assistant Experiment representative at JPL, who was responsible for most of the detailed sequencing of our experimental observations. We also acknowledge the efforts and operations of all Voyager Project personnel, who have made this mission a success. Kitt Peak National Observatory is operated by the Association of Universities for Research in Astronomy, Inc., under contract with the National Science Foundation. The research described in this report was carried out by the Jet Propulsion Laboratory, California Institute of Technology, under NASA contract NAS 7-100.

23 April 1979

Magnetic Field Studies at Jupiter by Voyager 1: Preliminary Results

Abstract. *Results obtained by the Goddard Space Flight Center magnetometers on Voyager 1 are described. These results concern the large-scale configuration of the Jovian bow shock and magnetopause, and the magnetic field in both the inner and outer magnetosphere. There is evidence that a magnetic tail extending away from the planet on the nightside is formed by the solar wind-Jovian field interaction. This is much like Earth's magnetosphere but is a new configuration for Jupiter's magnetosphere not previously considered from earlier Pioneer data. We report on the analysis and interpretation of magnetic field perturbations associated with intense electrical currents (approximately 5×10^6 amperes) flowing near or in the magnetic flux tube linking Jupiter with the satellite Io and induced by the relative motion between Io and the corotating Jovian magnetosphere. These currents may be an important source of heating the ionosphere and interior of Io through Joule dissipation.*

The Voyager magnetic field experiment consists of dual low field (LFM) and high field (HFM) triaxial fluxgate magnetometer sensors and associated electronics with extensive redundancy for high reliability as well as correction for the spacecraft's magnetic field (1). One LFM is located at the tip of a 13-m

boom; the other is mounted 5.6 m in-board. The total weight of the sensors plus electronics, including the two HFM instruments, is 5.6 kg, and the power required is 2.2 W. During encounter, the LFM's automatically ranged through seven (of eight possible) scales for maximum sensitivity [± 8.8 nanoteslas (nT)]